JVST B
Journal of Vacuum Science & Technology B

Photoassisted chemical smoothing of AlGaN surface after laser lift-off

Cite as: J. Vac. Sci. Technol. B **38**, 042207 (2020); https://doi.org/10.1116/6.0000192
Submitted: 14 March 2020 . Accepted: 22 June 2020 . Published Online: 10 July 2020

Zhongming Zheng, Hao Long, Samuel Matta, Mathieu Leroux, Julien Brault, Leiying Ying, Zhiwei Zheng, and Baoping Zhang

View Online Export Citation CrossMark

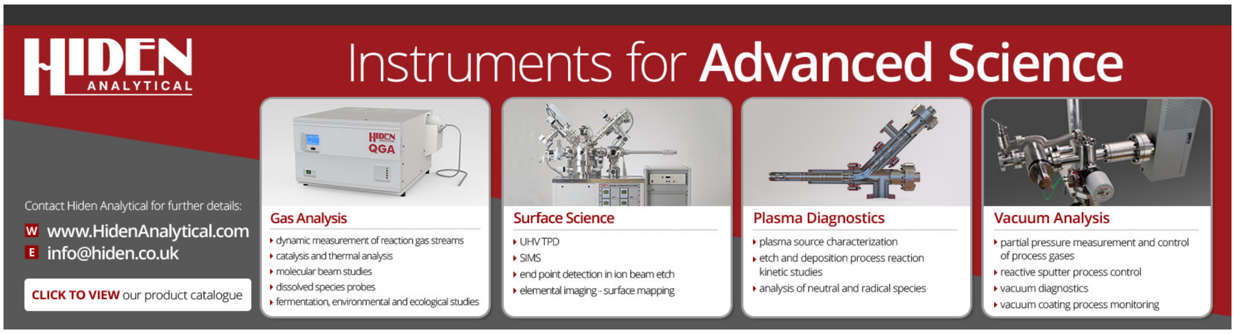

HIDEN ANALYTICAL
Instruments for **Advanced Science**

Contact Hiden Analytical for further details:
W www.HidenAnalytical.com
E info@hiden.co.uk
CLICK TO VIEW our product catalogue

Gas Analysis
- dynamic measurement of reaction gas streams
- catalysis and thermal analysis
- molecular beam studies
- dissolved species probes
- fermentation, environmental and ecological studies

Surface Science
- UHV TPD
- SIMS
- end point detection in ion beam etch
- elemental imaging - surface mapping

Plasma Diagnostics
- plasma source characterization
- etch and deposition process reaction kinetic studies
- analysis of neutral and radical species

Vacuum Analysis
- partial pressure measurement and control of process gases
- reactive sputter process control
- vacuum diagnostics
- vacuum coating process monitoring

© 2020 Author(s).

JVST B
Journal of Vacuum Science & Technology B

ARTICLE

avs.scitation.org/journal/jvb

Photoassisted chemical smoothing of AlGaN surface after laser lift-off

Cite as: J. Vac. Sci. Technol. B **38**, 042207 (2020); doi: 10.1116/6.0000192
Submitted: 14 March 2020 · Accepted: 22 June 2020 ·
Published Online: 10 July 2020

View Online Export Citation CrossMark

Zhongming Zheng,[1] Hao Long,[1,a)] Samuel Matta,[2] Mathieu Leroux,[2] Julien Brault,[2] Leiying Ying,[1]
Zhiwei Zheng,[1] and Baoping Zhang[1,b)]

AFFILIATIONS

[1] Department of Electronic Engineering, Optoelectronics Engineering Research Center, School of Electronic Science and Engineering (National Model Microelectronics College), Xiamen University, Xiamen 361005, Fujian, China
[2] Université Côte d'Azur, CNRS-CRHEA Centre de Recherche sur L'Hétéro-Epitaxie et ses Applications-Centre National de la Recherche Scientifique, Valbonne 06560, France

[a)] **Elecronic mail:** longhao@xmu.edu.cn
[b)] **Elecronic mail:** bzhang@xmu.edu.cn

ABSTRACT

To fabricate AlGaN-based ultraviolet (UV) vertical cavity surface-emitting laser diodes, a pair of distributed Bragg reflectors (DBRs) having a smooth surface is desired to have a high quality factor (Q). In this work, photoassisted chemical etching (PCE) was attempted to smoothen the -*c*(000-2) AlN surface after removing the sapphire substrate by means of the laser lift-off process. First, the conditions for PCE were optimized using an Xe lamp and KOH solution. The root-mean-square roughness of the -*c*(000-2) AlN surface was reduced from 30.5 to 5.6 nm, which enables us to fabricate an improved HfO_2/SiO_2 DBR on the AlN surface. Then, using the optimized PCE technique, improved UV (Al,Ga)N planar microcavities were fabricated and distinct cavity-mode-related emissions were observed using the photoluminescence (PL) technique. By comparing the PL spectra between the samples with and without PCE treatment, the Q value at 303 nm for the case of the improved DBR was determined to increase from 174 to 270. The increase in the Q value is mainly attributed to the reduction of scattering losses in optical cavities. Furthermore, the discussion on the mechanism of improved surface during the PCE treatment is given. Consequently, PCE is demonstrated to be a feasible approach to refine the quality of ultraviolet nitride microcavities.

Published under license by AVS. https://doi.org/10.1116/6.0000192

I. INTRODUCTION

Many recent research studies have been focused on improving the fabrication of deep ultraviolet (DUV) vertical cavity surface-emitting lasers (VCSELs).[1–6] In most of these studies, $Al_xGa_{1-x}N$ was used as the active layer. $Al_xGa_{1-x}N$ was chosen because it is a direct bandgap material with a bandgap ranging from 3.4 to 6.0 eV, depending on the Al concentration.[7] AlGaN has shown its prospect in DUV VCSEL; however, the results of these studies showed limitations, and improvements are needed to refine the quality of crystals and reduce defect densities. Moreover, the emission spectra were shown to switch from TE polarization to TM polarization at high-Al concentrations,[3,8] which may decrease the surface extraction efficiency. The quantum confinement Stark effect also decreases the internal quantum efficiency. In the fabrication of DUV planar microcavities by the laser lift-off (LLO) process, the rough surface induced by LLO causes severe optical scattering losses in the cavity, as reported in our previous work.[9] In that work, we fabricated a planar microcavity based on (Al,Ga)N quantum dots (QDs). However, the quality factor (Q) value of the cavity was only 167.[9] The main reason for the low Q value was the optical scattering losses at the rough surface interface after LLO. The epitaxial (Al,Ga)N film was separated from the sapphire substrate by LLO. After separation, the newly formed AlN surface was rough, which caused a large optical loss in the cavity. There are two approaches for improving the Q value: (a) placing the rough interface at the node of the optical field or (b) reducing the surface roughness after LLO. The former can be realized through the design of the cavity structures. For the latter, the surface can be smoothed by chemical mechanical polishing (CMP). However, it is difficult to control the CMP process with high precision in (Al,Ga)N, as high-Al (Al,Ga)N layers will curl after LLO due to the residual stress.

Published under license by AVS.

It has been reported that (Al,Ga)N can be etched in aqueous KOH.[10,11] During the etching process, the samples reacted with the solution directly. However, only N-face (Al,Ga)N reacted with KOH solution successfully.[10] Alternatively, (Al,Ga)N can be etched using an electrochemical cell.[12–21] Using this process, the (Al,Ga)N epilayer is masked with a patterned metal contact as the anode, along with an inert electrode as the cathode. KOH, HCl, HNO_3, and H_3PO_4 are all electrolytes that can be used in the solution. During the etching process, the epilayer was illuminated by a light such as an Xe lamp, whose photon energy was larger than the bandgap, to create electron-hole pairs. Holes were driven to the surface to facilitate the oxidation and dissolution of the surface by band bending or applied positive bias. Etching in KOH is relatively simpler without any additional metal contact or bias application needed, whereas using the electrochemical cell, the sample surface adjacent to the masked metal contact is etched preferentially, which results in nonuniform etching of the surface.[12,19]

In this work, the sample surface was smoothed by using a photoassisted chemical etching (PCE) method, as in KOH etching. The sample reacted with the KOH solution without a metal electrode, while an Xe lamp was used to enhance the etching. Different PCE conditions were evaluated to optimize AlN surface smoothing, and the smoothing mechanisms were also investigated. The atomic force microscope (AFM) measurement results showed that the root-mean-square (RMS) roughness of the AlN surface decreased from 30.5 to 5.6 nm, confirming the smoothing effects of PCE. A series of (Al,Ga)N QD planar microcavities were then fabricated on the smoothed surfaces. Photoluminescence (PL) results from the cavity showed that the Q value increased from 174 (without PCE) to 270 (with PCE).

II. EXPERIMENTAL METHODS

A. Experimental principle

Here, we briefly describe the experimental principle of PCE. During PCE, the (Al,Ga)N sample reacted with the KOH solution according to Eqs. (1)–(4).[10,11] The resulting NH_3 was able to be dissolved in water. Under Xe lamp illumination, holes were generated and accumulated on the sample surface due to surface band bending. It has been shown that photogenerated holes weaken the chemical bonds, promote etching, and increase the nitride etching rate.[12] Also, the sample surface was N-face, which would induce a positive polarization charge near the surface,[22] and attract OH^- from the liquid to the sample surface. After LLO, the surface was rough with many "pinnacle-shaped islands." This type of morphology increased the positive charge density on the top of the islands and attracted more OH^- and further increased the etch rate of the island structures,

$$2GaN + 3H_2O \xrightarrow{KOH} Ga_2O_3 + 2NH_3, \tag{1}$$

$$GaN + 3H_2O \xrightarrow{KOH} Ga(OH)_3 + NH_3, \tag{2}$$

$$2AlN + 3H_2O \xrightarrow{KOH} Al_2O_3 + 2NH_3, \tag{3}$$

$$AlN + 3H_2O \xrightarrow{KOH} Al(OH)_3 + NH_3. \tag{4}$$

B. Experimental setup

The epilayer structure is shown in Fig. 1(a). The GaN layer was used as a sacrificial layer for LLO. The active region was composed of $Al_{0.2}Ga_{0.8}N$ QDs sandwiched by $Al_{0.7}Ga_{0.3}N$ barrier layers. The epilayer was unintentionally doped and grown on a sapphire (0001) substrate by molecular beam epitaxy in a RIBER 32 P reactor.[23,24] The QD heights and diameters were 2.6 ± 0.3 and 10 ± 3 nm, respectively. To fabricate the VCSEL structure, a 15-pair HfO_2/SiO_2 (37.29 nm/50.17 nm) bottom distributed Bragg reflector (DBR) was first deposited on the sample surface. The sample was then inverted and transferred onto quartz. Then, the sapphire substrate was removed by LLO using a 248-nm KrF excimer laser. After LLO, the sample was soaked in an HCl solution to remove any metal (such as Ga and Al) from the surface. Then, the sample was separated into seven smaller pieces, designated samples A to G. PCE was performed on samples B–G at room temperature. A series of planar microcavities were fabricated by depositing a ten-pair HfO_2/SiO_2 top DBR on samples A–G. Fabrication steps are depicted in Fig. 1(b). The PCE experimental setup and conditions and total etching times for each sample are shown in Fig. 1(b) and Table I, respectively. During PCE, the samples were immersed in the KOH solution and exposed to Xe lamp illumination. The spectrum of the Xe lamp ranged from 200 to 1000 nm, and the upper value can generate electron-hole pairs in AlN. The light power was measured by a broadband power meter calibrated to 360 nm. During etching, the solution was not stirred, and the samples were etched in KOH, rinsed in de-ionized water, and dried

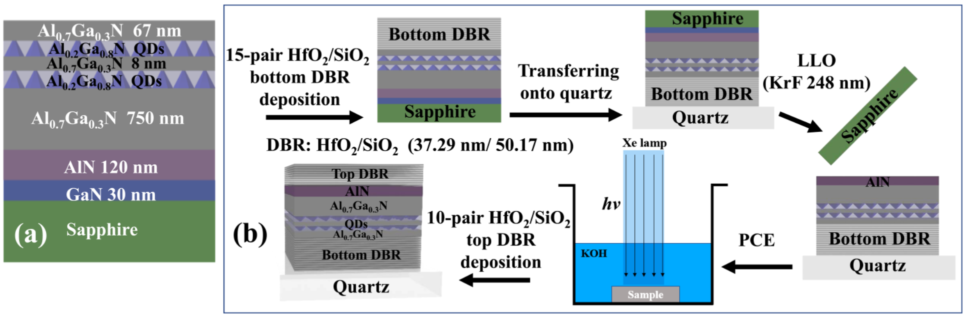

FIG. 1. (a) Epilayer structure of (Al,Ga)N QD-based samples. (b) Fabrication steps and experimental setup for PCE. A 15-pair HfO_2/SiO_2 bottom DBR was first deposited on the sample, followed by transferring onto quartz, LLO to remove the sapphire substrate, PCE to smoothen the sample surface, and deposition of a ten-pair HfO_2/SiO_2 top DBR.

Published under license by AVS.

TABLE I. PCE conditions for the sample series (A–G), including irradiation power density, KOH concentration, etching time, and surface RMS roughness of the samples.

Sample	KOH conc. ($\times 10^{-3}$ mol/l)	Irradiation intensity (W/cm^2)	Time (min)	RMS (nm)
A				30.5
B	2	1	12	~1000
C	0.5	1	12	~1000
D	0.3	1	96	29.3
E	0.2	1	96	26.3
F	0.3	0.5	96	5.6
G	0.3	0.2	96	51.5

with an air gun for several repeated cycles. Sample A was used as an unetched reference sample (i.e., without any PCE processing). Samples B–G were etched using different KOH concentrations and illumination intensities. The surface morphologies were measured using an AFM before (sample A) and after PCE (samples B–G). PL measurements were performed using a 266-nm Nd:YAG laser at room temperature.

III. RESULTS AND DISCUSSION

A. Results

The thickness of the GaN used as a sacrificial layer in the LLO process was 30 nm. Our previous work showed that nearly all the GaN is decomposed in the LLO process leaving only AlN.[25] The AFM image of sample A after LLO is shown in Fig. 2(a). It can be seen that there are many nanometer-sized islands on the surface. The heights of the islands varied from 73 to 296 nm, and the widths of the islands varied from 197 to 637 nm. The RMS roughness values were high, with a mean value of 30.5 nm.

For PCE smoothing, the KOH concentration was optimized first. Figures 3(a) and 3(b) are the surface images of samples B and C, respectively. They were treated with high concentrations of KOH, and their surfaces became very rough, which reached the AFM measuring range of 1 μm, after only 12 min of PCE treatment. Decreasing the KOH concentration to 0.3×10^{-3} mol/l, as in the case of sample D, smoothed the surface roughness smaller than 29.3 nm, after 12 min of etching. However, the surface was over-etched when the etching time was extended beyond 12 min, as shown in Fig. 2(b). Figure 2(b) shows the AFM image of sample D with 96-min PCE treatment, the RMS roughness is 29.3 nm. There are almost no islands; however, many holes can be seen in the surface, which indicated that the sample was overetched, and the light power density may have been too high to allow control of etching duration. When the concentration was further decreased to 0.2×10^{-3} mol/l, in the case of sample E, the surface morphology did not change significantly, even after 96 min of etching, as shown in Fig. 2(c). Figure 2(c) shows the AFM image of sample E with 96-min PCE treatment, the RMS roughness is 26.3 nm. There are also many islands on the surface, which indicated that the KOH concentration was too low for surface etching to occur. By comparing the results of samples B–E, we concluded that 0.3×10^{-3} mol/l KOH was the optimal concentration (sample D).

Next, the light power density was optimized. The light power density was reduced to 0.5 and 0.2 W/cm^2 for samples F and G,

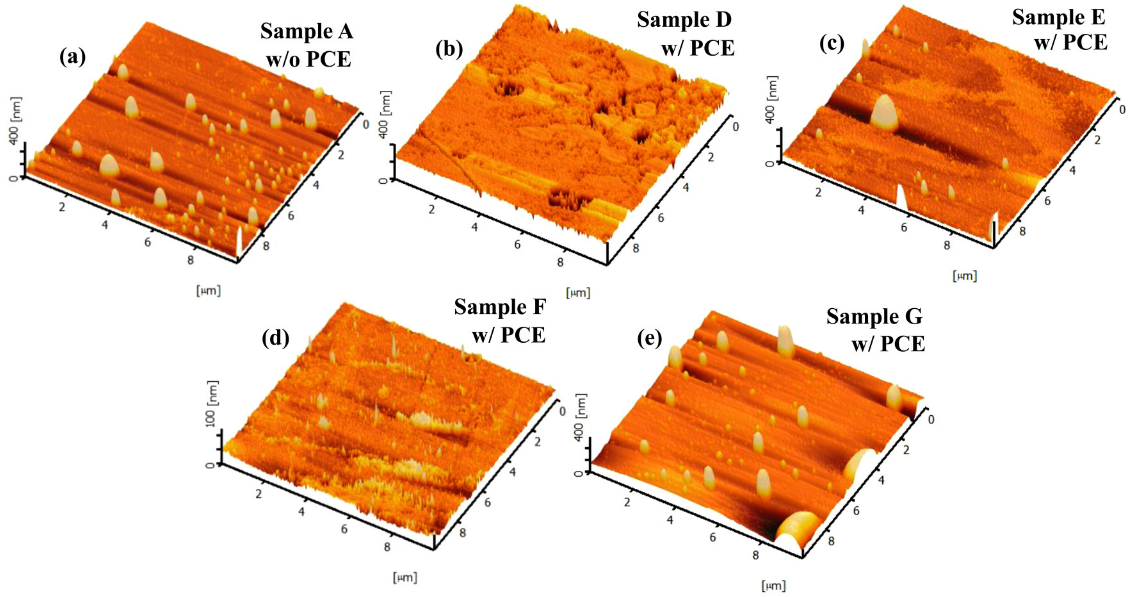

FIG. 2. AFM images ($10 \times 10\,\mu m^2$) of (a) sample A after the LLO process, and (b) sample D, (c) sample E, (d) sample F, and (f) sample G with PCE treatments. The surface RMS roughness values for each sample are 30.5, 29.3, 26.3, 5.6, and 51.5 nm, respectively.

Published under license by AVS.

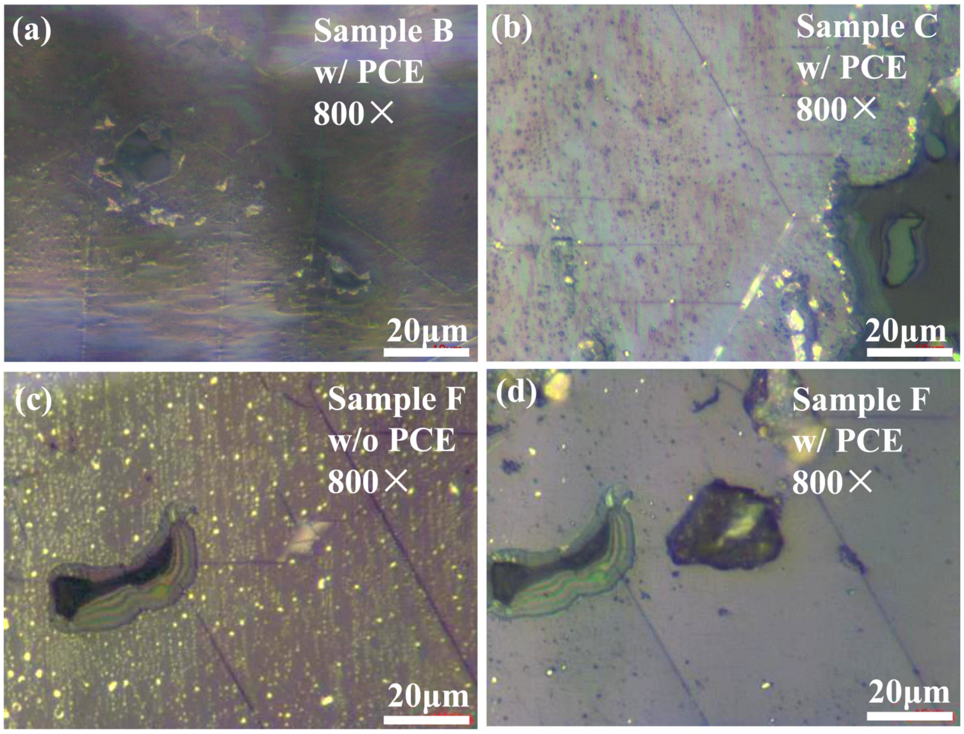

FIG. 3. Surface microscope images of (a) samples B and (b) C with PCE treatments, and sample F (c) without and (d) with PCE treatment.

respectively. Figures 3(c) and 3(d) show the surface microscope images of sample F before and after 96 min of PCE. Figure 2(d) shows the AFM image of sample F after 96 min of PCE. Before PCE, the surface of sample F was dense with islands [Fig. 3(c)]. After PCE, the surface morphology was significantly smoothed and some islands were no longer visible [Fig. 3(d)]. The AFM results [Fig. 2(d)] confirmed that the surface RMS roughness was significantly reduced to 5.6 nm, only 18% of the initial value. Figure 2(e) shows the AFM image of sample G after 96 min of PCE. The surface morphology did not change, with many islands, and the RMS roughness is 51.5 nm, even after 96 min of etching. This result indicated that the light intensity of 0.2 W/cm^2 was too weak for surface etching to occur. All the PCE conditions and RMS roughness for each sample are also listed in Table I.

The combined results of the KOH and light power density optimization experiments indicated that the optimal PCE conditions were 0.3×10^{-3} mol/l KOH with 0.5 W/cm^2 (at 360 nm) illumination. These conditions enabled the surface RMS roughness to decrease from 30.5 to 5.6 nm with no overetching within a PCE duration of 96 min.

After PCE, a ten-pair HfO_2/SiO_2 top DBR was deposited on samples A and F to complete fabrication of the DUV planar microcavities. PL measurements were performed on samples A and F. The results are shown in Fig. 4. Three cavity modes were observed for each of the two cavities. For sample A, the cavity modes were at 291, 303, and 317 nm, and the full width at half maximum (FWHM) was 1.75 nm (at 303 nm), as shown in Fig. 4(a). The Q value was calculated using the equation $Q = \Delta\lambda/\lambda$, where $\Delta\lambda$ is the FWHM of the cavity mode and λ is the center position of the cavity mode. The spectrum of the cavity mode was fitted with a Gaussian function to obtain the FWHM and center position. The Q value for sample A was 174, which was well in agreement with the value of 167 obtained in our previous work.[9] For sample F, cavity modes were at 290, 303, and 318 nm, and the FWHM was 1.12 nm (at 303 nm), as shown in Fig. 4(b). The Q value for sample F was 270, higher than that of sample A. These results demonstrate that the smoothing effect of PCE is effective for obtaining high Q values and low-loss microcavities.

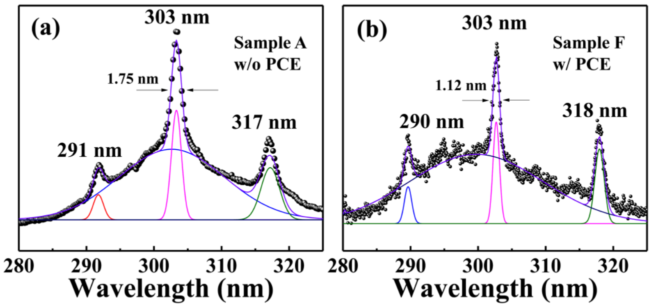

FIG. 4. Room temperature PL spectra of planar-cavities formed using (a) samples A and (b) F. The dots denote the experimental results, and the different lines denote the fitting results.

Published under license by AVS.

B. Discussion

In this section, we discuss the mechanisms of surface smoothing by PCE. Before the PCE experiment, the sample was determined to be N-polar after LLO by using a hot KOH solution etching method, which indicated that the sample could be easily etched in a KOH solution.[10] The surface smoothing was attributed to two factors: (a) the existence of islands on the sample surface after LLO and (b) repeated periods of etching the sample in KOH, rinsing in de-ionized water, and drying by an air gun.

1. Role of surface islands in PCE mechanism

The sample was N-polar after LLO, whose spontaneous polarization would induce a positive polarization charge at the surface.[22] Then, OH^- in the liquid would be attracted to the surface and start the etching reaction. Based on this principle, a simple model was proposed to simulate the electric potential lines and electric field on islands. This model was set up as follows: a rough AlN epilayer with many cones on the top surface was immersed in water. To simulate the spontaneous polarization and the corresponding internal electric fields, a positive voltage of +0.2 V was applied on the top surface of the epilayer. The bottom surface of the epilayer and water were grounded (0 V). Only relative dielectric constant was considered for all the material in the model [8.5 for AlN (Ref. 26) and 81 for water]. The simulation results were calculated using electrostatic field equations:

$$\nabla \cdot \boldsymbol{D} = \rho_V, \tag{5}$$

$$\boldsymbol{E} = -\nabla V, \tag{6}$$

where $\boldsymbol{D}$ is the electric displacement vector, ρ_v is the charge density, $\boldsymbol{E}$ is the electric field, and V is the electric potential. Figure 5(a) shows the simulation results of electric potential lines and electric field. It is clear that, in water but outside of the island, the electric field will lead OH^- to the island and increase the etching rate, so the island can be preferentially etched. The unintentionally doped nitride is usually n-type, and the band bends upward near the surface,[27–29] as shown in Fig. 5(b), which is also the band diagram of sample F near the surface. Under above-bandgap illumination, holes were generated and then drifted to the surface by band bending. Inside the island, the electric field at the top of the island was weaker than that at the bottom, which indicated the lower positive charge density at the top of the island. This resulted in higher upward band bending at the top of the island than at the bottom, which caused the holes to drift to the top of the island. Holes could weaken the chemical bonds and promote etching,[12] causing the islands to be preferentially etched further. The results presented in Fig. 2 demonstrate this phenomenon. A comparison of Figs. 2(a) and 2(d) shows that the island size decreases after PCE, indicating that the preferential etching of islands was demonstrated by PCE.

2. Role of etching, rinsing, and drying cycles in the PCE mechanism

High-speed water flow is expected to remove some insoluble products, such as Al_2O_3 and $Al(OH)_3$. However, the KOH concentration may have been too low to dissolve them, and Al_2O_3 and $Al(OH)_3$ can obstruct the etching process. Al_2O_3 and $Al(OH)_3$ would cover the surface of sample and lower or stop the PCE process. It should be mentioned that the KOH solution was not stirred during etching, so that OH^- could be successfully attracted to the islands.

Some similar studies have focused on the treatment of (Al,Ga)N surfaces by chemical etching. However, surface roughness was found to be increased in these studies rather than decreased. Youtsey *et al.* reported that when n-GaN was chemically etched, the RMS roughness of the surface increased from 0.3 to 1.5 nm.[19] Stocker and Schubert also reported on chemical etching of GaN, where the RMS roughness of the surface increased from 17 to 20 nm.[16] In comparison, the PCE process in this study resulted in smoothing of the (Al,Ga)N surface, with the RMS roughness decreasing from 30.48 to 5.6 nm. The reaction mechanism in our experiment also was different than those in the referenced studies, which used electrochemical cells, as was described in the Introduction section. The reaction function in the study by Youtsey

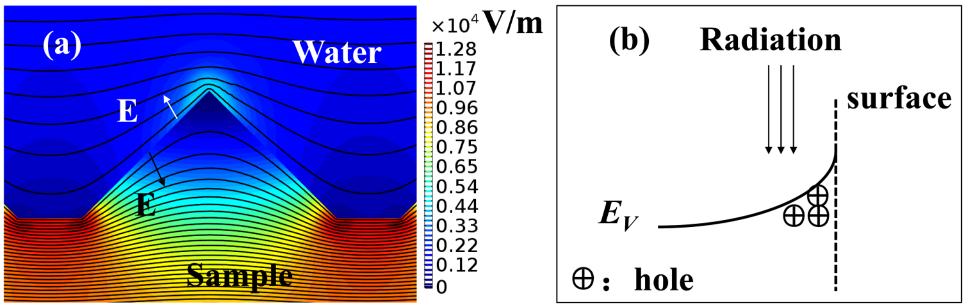

FIG. 5. (a) Simulation results of electric potential lines and electric field near islands of the sample after LLO. The pyramid represents the island, the black bold lines are electric potential lines, and the arrows show the electric field direction. Inside the island, the electric field at the top is weaker than that at the bottom. In water but out of the island, the electric field at top of island is stronger than that at the bottom. (b) Common band diagram near the sample surface of n-type nitride, which is also the surface band diagram of sample F.

Published under license by AVS.

et al. is shown in Eq. (7) (Ref. 14) below and the functions in the study by Stocker and Schubert are shown in Eqs. (8) and (9). Metal contacts were masked on the samples in both studies, and an inert counter electrode also was used in each case. Results suggested that the surface adjacent to the masked contacts was preferentially etched,[12,19] which could be attributed to higher etchant concentration in those regions. In those cases, the rough areas were not preferentially etched. In our experiment, a simple method with no additional bias or electrode was proposed and demonstrated, and the rough areas were preferentially etched,

$$2\mathrm{GaN} + 6h^{+} \longrightarrow 2\mathrm{Ga}^{3\,+} + \mathrm{N}_2 \uparrow, \tag{7}$$

$$2\mathrm{GaN} + 6h^{+} + 6\mathrm{OH}^{-} \longrightarrow \mathrm{Ga}_2\mathrm{O}_3 + \mathrm{N}_{2-} + 3\mathrm{H}_2\mathrm{O} \qquad \text{(at the anode)}, \tag{8}$$

$$6\mathrm{H}^{+} \longrightarrow 3\mathrm{H}_2 \uparrow + 6h^{+} \qquad \text{(at the cathode)}. \tag{9}$$

IV. CONCLUSION

In summary, we proposed using PCE as a simple, feasible method of smoothing AlN surfaces after laser lift-off. The optimal experimental conditions were found to be a 0.3×10^{-3} mol/l KOH solution with 0.5 W/cm^2 (at 360 nm) illumination. The surface RMS roughness was decreased from 30.5 to 5.6 nm by adding the PCE step. Planar microcavities were fabricated on the smoothed surfaces and Q values were increased from 174 to 270 using optimized PCE conditions. These results show that PCE processes can be used to smooth nitride-based semiconductors for the fabrication of deep ultraviolet microcavities.

ACKNOWLEDGMENTS

This work was supported by the Science Challenge Project (Grant No. TZ2016003), the National Key R&D Program of China (Grant Nos. 2016YFB0400803 and 2017YFE0131500), the National Natural Science Foundation of China (NNSFC) (Grant No. 61704140), and the Natural Science Foundation of Fujian Province of China (No. 2019J05023). Julien Brault, Samuel Matta, and Mathieu Leroux acknowledge partial support from the ANR Project <ANR-14-CE26-0025> "NANOGANUV."

REFERENCES

[1] Joan M. Redwing, David A. S. Loeber, Neal G. Anderson, Michael A. Tischler, and Jeffrey S. Flynn, Appl. Phys. Lett. **69**, 1 (1996).
[2] Hailong Zhou, M. Diagne, E. Makarona, and A. V. Nurmikko, Electron. Lett. **36**, 1777 (2000).
[3] X. H. Li *et al.*, Appl. Phys. Lett. **106**, 041115 (2015).
[4] Yuh-Shiuan Liu, Tsung-Ting Kao, Karan Mehta, Shyh-Chiang Shen, P. Douglas Yoder, Theeradetch Detchprohm, Russell D. Dupuis, Hongen Xie, and Fernando A. Ponce, Proc. SPIE **9748**, 974815 (2015).
[5] Yuh-Shiuan Liu *et al.*, Appl. Phys. Express **9**, 111002 (2016).
[6] Young Jae Park *et al.*, Proc. SPIE **10938**, 109380A (2019).
[7] M. Leroux *et al.*, Phys. Status Solidi B **234**, 887 (2002).
[8] T. Detchprohm, Xiaohang Li, S.-C. Shen, P. D. Yoder, and R. D. Dupuis, Semicond. Semimetals **96**, 121 (2017).
[9] Zhongming Zheng *et al.*, J. Nanophoton. **12**, 043504 (2018).
[10] W. Guo, R. Kirste, I. Bryan, Z. Bryan, L. Hussey, P. Reddy, J. Tweedie, R. Collazo, and Z. Sitar, Appl. Phys. Lett. **106**, 082110 (2015).
[11] Dongsheng Li, M. Sumiya, S. Fuke, Deren Yang, Duanlin Que, Y. Suzuki, and Y. Fukuda, J. Appl. Phys. **90**, 4219 (2001).
[12] J. E. Borton, C. Cai, M. I. Nathan, P. Chow, J. M. Van Hove, A. Wowchak, and H. Morkoc, Appl. Phys. Lett. **77**, 1227 (2000).
[13] L. H. Peng, C. W. Chuang, Y. C. Hsu, J. K. Ho, C. N. Huang, and C. Y. Chen, Appl. Phys. Lett. **72**, 939 (1998).
[14] C. Youtsey, I. Adesida, and G. Bulman, Appl. Phys. Lett. **71**, 2151 (1997).
[15] P. Visconti, M. A. Reshchikov, K. M. Jones, D. F. Wang, R. Cingolani, H. Morkoçˇ, R. J. Molnar, and D. J. Smith, J. Vac. Sci. Technol. B **19**, 1328 (2001).
[16] D. A. Stockerz and E. F. Schubert, J. Electrochem. Soc. **146**, 2702 (1999).
[17] E. D. Haberer, R. Sharma, A. R. Stonas, S. Nakamura, S. P. DenBaars, and E. L. Hu, Appl. Phys. Lett. **85**, 762 (2004).
[18] M. S. Minsky, M. White, and E. L. Hu, Appl. Phys. Lett. **68**, 1531 (1996).
[19] C. Youtsey, I. Adesida, L. T. Romano, and G. Bulman, Appl. Phys. Lett. **72**, 560 (1998).
[20] A. C. Tamboli, M. C. Schmidt, S. Rajan, J. S. Speck, U. K. Mishra, S. P. DenBaars, and E. L. Hu, J. Electrochem. Soc. **156**, H47 (2009).
[21] C. Youtsey *et al.*, Phys. Status Solidi B **254**, (2017).
[22] M. Stutzmann *et al.*, Phys. Status Solidi B **228**, 505 (2001).
[23] S. Matta *et al.*, J. Appl. Phys. **122**, 085706 (2017).
[24] J. Brault *et al.*, Semicond. Sci. Technol. **33**, 075007 (2018).
[25] Ming Chen, Jiang-Yong Zhang, Xue-Qin Lv, Lei-Ying Ying, and Bao-Ping Zhang, Chin. Phys. Lett. **30**, 014203 (2013).
[26] Fabio Bernardini, Vincenzo Fiorentini, and David Vanderbilt, Phys. Rev. B **56**, R10024(R) (1997).
[27] Ho Won Jang, Jung-Hee Lee, and Jong-Lam Lee, Appl. Phys. Lett. **80**, 3955 (2002).
[28] Yow-Jon Lin, Yow-Lin Chu, Wen-Xiang Lin, Feng-Tso Chien, and Chi-Sen Lee, J. Appl. Phys. **99**, 073702 (2006).
[29] Brianna S. Eller and Robert J. Nemanich, J. Appl. Phys. **122**, 125304 (2017).

Published under license by AVS.